Contribution from the Fachbereich Chemie der Philipps-Universität, D-3550 Marburg/Lahn, FRG, and Lehrstuhl für Anorganische Chemie I der Ruhr-Universität, D-4630 Bochum, FRG

Spectroscopic and Magnetic Properties of Pseudooctahedral Cu^{2+} and Co^{2+} Complexes with 1,4,7-Triazacyclononane and Its Monooxa and Trithia Analogues as Ligands

Dirk Reinen,*† Andrzej Ozarowski,†‡ Bernd Jakob,† Jürgen Pebler,† Horst Stratemeier,† Karl Wieghardt,*§ and Ingolf Tolksdorf§

Received October 2, 1986

The bonding properties of pseudooctahedral transition-metal complexes with the cyclic tridentate 1,4,7-triazacyclononane and its monooxa and trithia analogues as ligands have been studied on the basis of spectroscopic and magnetic data. For Cu^{2+} and low-spin Co^{2+} strong tetragonal Jahn-Teller distortions are found; the transition to the dynamically averaged octahedra usually covers a wide temperature range. Co^{2+} is stabilized in the low-spin state by the trithia and monooxa diaza ligands, with a doublet-quartet separation in the range of thermal energies in the latter case. The trithia ligand is more covalent than the triaza ligand, though the Δ parameters are nearly equivalent. An analysis utilizing the angular-overlap model is given. Bonding parameters have been derived from the EPR hyperfine structures in frozen solution.

Introduction

A large number of pseudooctahedral complexes with the tridentate ligand 1,4,7-triazacyclononane (TACN) and divalent and trivalent 3d transition-metal ions have been prepared so far, while only a few examples of complexes with the trithia analogue (TTCN) as ligand are reported in the literature. Also, data on bonding properties are scarce for ligands with sulfur ligator atoms, and it seemed attractive for us to compare the two ligands in this respect. We will further include in the discussion the 1-oxa-4,7-diazacyclononane ligand (ODACN), which was promising

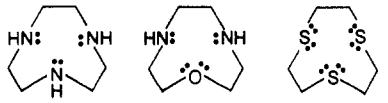

TACN ODACN TTCN

regarding the Co^{2+} complexes. The three ligands may stabilize either the high- or low-spin configuration for Co^{2+} and even induce temperature-dependent high-spin-low-spin equilibria. We have collected EPR data in the solid and in frozen solution in dependence on temperature for a variety of Cu^{2+} and Co^{2+} complexes and, together with the optical spectra and magnetic results, interpreted them in terms of bonding parameters. The stability of complexes with the tridentate ligands is remarkably high because of the entropy contribution to the Gibbs free energy.[1] Optical spectra for Ni^{2+} have been reported in the literature and will shortly be considered for reasons of comparison with Co^{2+} and Ni^{2+}.

TACN is a pure σ donor comparable to NH_3 and ethylenediamine (en). The ligand field parameters, calculated from the observed d-d bands of Ni^{II} complexes[2] with σ-donor ligands, demonstrate that $\Delta = 3e_\sigma$ becomes larger by about 20% in the sequence from NH_3 to triazacyclononane (Table I), which may be explained by the increasing number of secondary nitrogen atoms with stronger base properties. The $B_{55} \simeq B_{35}$[3] parameters ($\simeq$865 cm^{-1}) and the corresponding nephelauxetic ratios ($\simeq$0.83) are nearly identical within the experimental error limit (Table I). The B_{33} value,[3] calculated from the $^3A_{2g} \rightarrow {}^1_aE_g$ band in the spectrum of the $Ni(TACN)_2^{2+}$ complex with $C/B \simeq C_0/B_0 = 4.2$,[4] is much lower (B_{33} = 730 cm^{-1}). It results from a transition within the ground-state $t_{2g}^6e_g^2$ configuration and hence reflects the σ-covalence more strongly than the intermixed $t_{2g}^6e_g^2 \rightarrow t_{2g}^5e_g^3$, $t_{2g}^4e_g^4$ main transitions $^3A_{2g} \rightarrow {}^3_aT_{1g}$, ${}^3_bT_{1g}$, which give rise to B_{35} and B_{55}. For the analogous pseudooctahedral terpyridine complexes a comparable Δ parameter (12 400 cm^{-1}) but a significantly lower B_{33} (660 cm^{-1}) and $B_{35} \simeq B_{55}$ value ($\sim$700 cm^{-1}, estimated from the $^3A_{2g} \rightarrow {}^3_aT_{1g}$ band) are reported.[5] Presumably an increased covalency of the Ni-N bond in $Ni(terpy)_2^{2+}$, with a slightly larger e_σ parameter than for $Ni(TACN)_2^{2+}$ and a finite e_π energy, has induced the smaller nephelauxetic parameters. The nitro ligand, for which SCF-MO calculations suggest only small π interactions with Cu^{2+} for example,[6] induces similar Δ (13 000 $\pm$ 800 cm^{-2}) and B_{33} parameters (730 cm^{-1}) in Ni^{2+} complexes.[7] Unfortunately, $B_{35} \simeq B_{55}$ cannot be measured in these cases, because the d-d transitions to the $a,{}^3_bT_{1g}$ states are masked by charge-transfer bands.

Table I. Ligand Field Parameters for Octahedral Ni^{2+} Complexes with σ-Donor Ligands (10^3 cm^{-1}), Calculated from Ligand Field Data[a]

Δ	$B_{35} \cong B_{55}$	β^b	e_σ	ligand
10.8	0.89	0.85_5	3.6	NH_3
11.6	0.84	0.81	3.9	en
12.6	0.86	0.82_5	4.2	TACN

[a] Collected in ref 2, for example. [b] $\beta = B/B_0$ with B_0 = 1040 cm^{-1} and $B = B_{35} \cong B_{55}$.

For $[Ni(ODACN)_2]^{2+}$ complexes it is suggested that the oxygen ligator atoms occupy trans positions.[8] Δ values are reported,[9] which are about 1000 cm^{-1} smaller than those of the corresponding triaza compounds (Table I)-in good agreement with the weighted average between the ligand field parameters of the latter complexes and hexaoxa-coordinated compounds ($\simeq$8500 cm^{-1}). The reported B value (820 cm^{-1})[9] is also decreased with respect to the one for the triaza complex (Table I). The reflection spectrum of $[Ni^{II}(TTCN)_2](ClO_4)_2$ shows three main bands at 12 600, 19 700, and 30 200 cm^{-1}, yielding Δ = 12 600 cm^{-1} and $B_{35} \simeq B_{55}$ = 800 cm^{-1}. The weak shoulder at $\simeq$11 700 cm^{-1} can be assigned to the $^3A_{2g} \rightarrow {}^1_aE_g$ transition and leads to B_{33} = 740 cm^{-1}—practically identical with the value for the triaza ligand. For the solution spectrum slightly different parameters (Δ = 12 750 cm^{-1}, B = 780 cm^{-1}) are reported.[10] Apparently the Δ value is about the same as for the triaza ligand, while $B_{35} \simeq B_{55}$ is significantly lower (Table I), indicating a higher degree of covalency of the Ni-S

† Philipps-Universität Marburg.
‡ On leave from the Institute of Chemistry, Wroclaw University, Wroclaw, Poland.
§ Ruhr-Universität Bochum.

(1) Hancock, R. D.; McDougall, G. J. *J. Am. Chem. Soc.* **1980**, *102*, 5661.
(2) Lever, A. B. P. *Inorganic Electronic Spectroscopy*; Elsevier: Amsterdam, 1984.
(3) Jørgensen, C. K. *Modern Aspects of Ligand Field Theory*; North-Holland: Amsterdam, 1971.
(4) Reinen, D. *Theor. Chim. Acta* **1966**, *312*, 5.
(5) Henke, W.; Reinen, D. *Z. Anorg. Allg. Chem.* **1977**, *436*, 187.
(6) Clack, D. W.; Reinen, D. *Solid State Commun.* **1980**, *34*, 395.
(7) Reinen, D.; Friebel, C.; Reetz, K. P. *J. Solid State Chem.* **1972**, *4*, 103. Grefer, J.; Reinen, D. *Z. Anorg. Allg. Chem.* **1974**, *404*, 167.
(8) Boeyens, J. C. A.; Hancock, R. D.; Thörm, V. J. *J. Crystallogr. Spectrosc. Res.* **1984**, *14*, 261.
(9) Yang, R.; Zompa, L. J. *Inorg. Chem.* **1976**, *15*, 1499. Zompa, L. J. *Inorg. Chem.* **1978**, 17, 2531. Nonoyama, M. *Transition Met. Chem. (Weinheim, Ger.)* **1976**, *1*, 70. Zompa, L. J.; Margulis, T. N. *Inorg. Chim. Acta* **1978**, *28*, L157.
(10) Wieghardt, K.; Küppers, H. J.; Weiss, J. *Inorg. Chem.* **1985**, *24*, 3067.

0020-1669/87/1326-4010$01.50/0 © 1987 American Chemical Society

bond (see below). In contrast to the case for TACN the spectral parameters are expected to reflect also π-donor properties in the case of the TTCN ligand. Charge-transfer bands occur above 30 000 cm^{-1}, and hence even the third d–d band is partly resolved.

Experimental Section

Preparation. The ligands 1,4,7-triazacyclononane (TACN, $C_6H_{15}N_3$)[11] and 1,4,7-trithiacyclononane (TTCN, $C_6H_{12}S_3$)[12] were prepared according to procedures described in the literature. 1-Oxa-4,7-diazacyclononane (ODACN) has been synthesized by following the procedures described by Vögtle et al.[13] and Hancock et al.[1] Since the detosylation reaction of *N,N'*-bis(*p*-tolylsulfonyl)-4,7-diaza-1-oxacyclononane with concentrated H_2SO_4 leads to <20% yields of the dihydrosulfate due to ether cleavage reactions, we have employed an alkaline, reductive detosylation method. *N,N'*-Bis(*p*-tolylsulfonyl)-4,7-diaza-1-oxacyclononane (110 g, 0.25 mol) was suspended in a mixture of *n*-butanol (800 mL) and di-*n*-butyl ether (600 mL) and heated to 130 °C. Sodium (63.3 g, 2.75 mol) was added in small amounts within 6 h, during which time the solution was gently refluxed. The solution was then stirred at 130 °C for 18 h. To the cooled solution was added concentrated hydrochloric acid (350 g) in small amounts. After dilution with water (150 mL) the suspension was stirred at room temperature overnight. All solvents were removed under reduced pressure, and the residue was dissolved in boiling water (1500 mL) and the mixture filtered. To the filtrate was added sodium hydroxide (40 g, 1 mol), and the water was removed by azeotropic distillation with benzene. After removal of the benzene under reduced pressure the residue was extracted three times with dry, hot benzene. After the benzene was removed under reduced pressure, the resulting brown oil was distilled over a 12-cm Vigreux column. The pale yellow fraction between 123 and 127 °C at 7.8 mbar was collected (yield 55%).

The complexes **$[Co(TACN)_2]I_2 \cdot 2H_2O$, $[Cu(TTCN)_2](ClO_4)_2$, and $[Co(TTCN)_2](ClO_4)_2$** have been prepared as described previously.[14]

$[Co(ODACN)_2](ClO_4)_2$. A deoxygenated aqueous solution of $CoCl_2 \cdot 6H_2O$ (0.95 g, 4 mmol) and 1-oxa-4,7-diazacyclononane (1.04 g, 8 mmol) was stirred for 45 min at 50 °C, and $NaClO_4 \cdot H_2O$ (10 g) was added. When the mixture was cooled, light red-brown crystals precipitated, which were filtered off and recrystallized from a minimum amount of perchloric acid (pH ≃4) (yield 53%). Anal. Calcd for $C_{12}H_{28}N_4O_{10}Cl_2Co$: C, 27.81; H, 5.45; N, 10.81; Co, 11.37; ClO_4, 38.38. Found: C, 27.8; H, 5.4; N, 10.7; Co, 11.8; ClO_4, 38.2. The diiodide (dibromide) salt was prepared from an aqueous solution of the above perchlorate salt by addition of sodium iodide (bromide).

$[Cu(ODACN)_2]Br_2$. This blue complex was prepared analogously to $[Co(ODACN)_2](ClO_4)_2$, with use of $CuCl_2 \cdot 4H_2O$ as starting material and NaBr for precipitation. Anal. Calcd for $C_{12}H_{28}N_4O_2Br_2Cu$: Cu, 29.80; H, 5.83; N, 11.58; Br, 33.04. Found: C, 29.7; H, 5.7; N, 11.6; Br, 32.9.

Spectroscopic and Magnetic Measurements. The diffuse-reflectance spectra between 4000 and 25 000 cm^{-1} at 298 and 5 K as well as the solution spectra have been recorded by a Zeiss PMQ II spectrophotometer (with a low-temperature accessory). The EPR measurements between 298 and 4.2 K were performed with a Varian E 15 spectrometer at X- and Q-band frequencies. DPPH was used as internal standard.

A Foner magnetometer with a cryostat was used for taking the magnetization data between 4.2 and 298 K (calibration with $Hg[Co(NCS)_4]$). Supplementary susceptibility measurements were also performed by using the Faraday method (Sartorius microbalance, Bruker B-E 1008 research magnet, and Bruker B-VT 1000 automatic temperature control). Diamagnetic corrections were applied with use of Pascal's constants.

Results and Discussion

I. Cu^{2+} Ligand Field Spectra. The $[Cu(TACN)_2]^{2+}$ complex in $[Cu^{II}(TACN)_2]Cu^{I}(CN)_3 \cdot 2H_2O$ exhibits a strong Jahn–Teller distortion corresponding to a tetragonal elongation, which is (partly) dynamic above ≃120 K, however.[15] The two bands in the reflectance spectrum at 7800 and 16 300 cm^{-1} (also for the perchlorate salt; Figure 1, spectrum II) are assigned to the transitions $^2B_{1g}(^2E_g) \rightarrow {}^2A_{1g}(^2E_g)$ (Jahn–Teller splitting of the σ-antibonding ^2E_g ground state in O_h symmetry) and $^2B_{1g}(^2E_g) \rightarrow {}^2B_{2g}, {}^2E_g(^2T_{2g})$, respectively. The latter band is not split within the experimental band width, because the $^2T_{2g}$ parent state is nonbonding. The assignment is consistent with the data of other octahedral Cu^{2+} compounds[16] and the corresponding Ni^{2+} and Co^{2+} complexes (see below). The two transitions correspond to the AOM energies

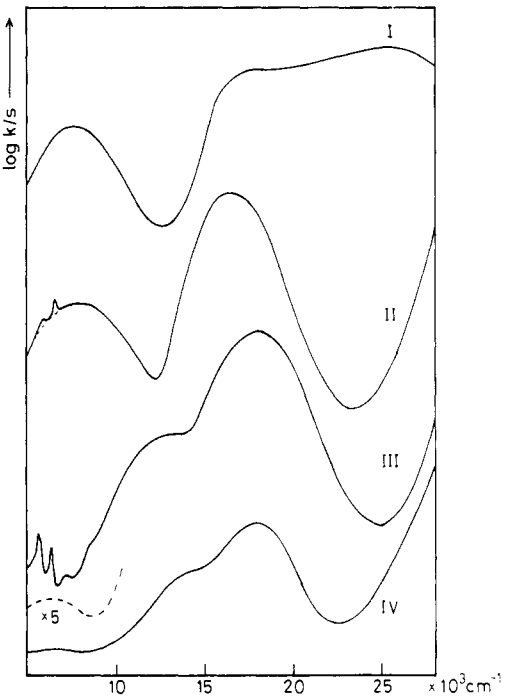

Figure 1. Ligand field reflectance (I–III) and solution spectra (IV) of complexes $[CuL_2]X_2$: (I) L = TTCN, X = ClO_4^-; (II) L = TACN, X = ClO_4^-; (III) L = ODACN, X = Br; (IV) L = ODACN, X = Br in H_2O (between 500 and 8000 cm^{-1} the average over the extensive fine structure in this energy region is shown).

$$4E_{JT} = 2(e_\sigma^s - e_\sigma^l) + E_{ds} \qquad E_{T_2} = 3e_\sigma^s \tag{1}$$

where e_σ^s (=5400 cm^{-1}) correlates with the four short (a_s = 2.06 Å) and e_σ^l (=2800 cm^{-1}) with the two long Cu–N spacings (a_l = 2.32 Å) in the tetragonally elongated octahedron. E_{ds} (=2600 cm^{-1}) is an energy contribution resulting from the interaction of the $^2A_{1g}$ state with a term of the same symmetry, originating from the 4s orbital of Cu^{2+}.[17] e_σ^l was calculated from e_σ^s, by using the relation $e_\sigma = K_\sigma S_\sigma^2$ and tabulated overlap integrals.[18] Similarly the energy parameter for the average (octahedral) Cu–N bond length ($\bar{a}$ = 2.14 Å) can be estimated: $e_\sigma^0 = [S(\bar{a})^2/S(a_s)^2]e_\sigma^s \simeq 4400\ cm^{-1}$. This value resembles those of Ni^{2+} (Table I) and Co^{2+} (see below)—as expected for transition elements of the same series with the same oxidation state and similar d-electron numbers and ionic radii. The extent of the distortion of the CuN_6 polyhedron can be expressed by the radial distortion parameter ρ[16]

$$\rho = [\sum_i 2(\Delta a_i)^2]^{1/2} \qquad i = x, y, z \tag{2}$$

where the Δa_i values are the deviations of the copper–ligand spacings from the average bond length $\bar{a}$. $\bar{a}$ (2.14 Å) and ρ (0.30 Å) are nearly identical with the values of the corresponding $Cu(terpy)_2^{2+}$ polyhedron in the nitrate salt ($\bar{a}$ = 2.14 Å, ρ = 0.31 Å).[19] The ground-state splitting for the latter compound ($4E_{JT}$ = 7350 cm^{-1})[5] is also comparable to that for $[Cu(TACN)_2]$-

(11) Atkins, T. J.; Richman, J. E.; Oettle, W. F. *Org. Synth.* **1978**, *58*, 86. Wieghardt, K.; Schmidt, M.; Nuber, B.; Weiss, J. *Chem. Ber.* **1979**, *112*, 2220.
(12) Sellmann, D.; Zapf, L. *Angew. Chem.* **1984**, *96*, 799; *Angew. Chem., Int. Ed. Engl.* **1984**, *23*, 807; *J. Organomet. Chem.* **1985**, *289*, 57.
(13) Rasshofer, W.; Wehner, W.; Vögtle, F. *Justus Liebigs Ann. Chem.* **1976**, 916.
(14) Küppers, H. J.; Neves, A.; Pomp, C.; Ventur, D.; Wieghardt, K.; Nuber, B.; Weiss, J. *Inorg. Chem.* **1986**, *25*, 2400.
(15) Chaudhuri, P.; Oder, K.; Wieghardt, K.; Weiss, J.; Reedijk, J.; Hinrichs, W.; Wood, J.; Ozarowski, A.; Stratemeier, H.; Reinen, D. *Inorg. Chem.* **1986**, *25*, 2951.
(16) Reinen, D.; Friebel, C. *Struct. Bonding (Berlin)* **1979**, *37*, 1.
(17) Hitchman, M. A.; Cassidy, P. J. *Inorg. Chem.* **1979**, *18*, 1745.
(18) Smith, D. W. *Struct. Bonding (Berlin)* **1979**, *12*, 49.
(19) Allmann, R.; Henke, W.; Reinen, D. *Inorg. Chem.* **1978**, *17*, 378.

Table II. Q-Band EPR Data (Hyperfine Tensor Components in 10^{-4} cm^{-1}) and Parameters of the Complexes $[Cu^{II}(TACN)_2][Cu^{I}(CN)_3]$ (I), $[Cu^{II}(ODACN)_2]Br_2$ (II), and $[Cu^{II}(TTCN)_2](ClO_4)_2$ (III) in DMF or DMSO Solution (Isotropic, 298 K) and Solid Solution (130 K)[a]

	$g_\parallel$	$g_\perp$	$A_\parallel$	$A_\perp$[d]	A_{iso}	g_{iso}	k	α
I[15]	2.22_9	2.05_5	−177	−22	−75	2.11	0.75_5	0.86_5
II	2.20_5[c]	≃2.04[c]	−198	−27	−83	2.10_5	0.75_5	0.87_5
	[≃2.28	≃2.06	−182	−25	...	...	...	$0.90]$[e]
III	2.11_4[b]	2.02_7[b]	−153[b]	−20	−62[f]	2.06[f]	≃0.55	0.74

[a] k = covalency factor, from the g tensor; α = mixing coefficient of $d_{x^2-y^2}$ in the ground-state MO, from hyperfine tensor A. [b] 4.2 K. [c] Powder spectrum (130 K): 2.20_4, 2.05_0, 2.04_5. [d] Calculated values (see text). [e] Additional species (see text). [f] In H_2O at 280 K.

$Cu^I(CN)_3 \cdot 2H_2O$ and indicates rather similar e_σ parameters in both complexes. On the other hand, the second ligand field transition is found at 14 850 cm^{-1} for the terpyridine ligand,[5] which is about 1500 cm^{-1} lower than for TACN. Obviously the octahedral T_{2g} state is weakly π antibonding and hence slightly reduced in energy with respect to the nonbonding situation for the triazacyclononane ligand. Copper(II) nitro complexes $A^I_2B^{II}Cu(NO_2)_6$ (A^I = Cs, Rb, K, Tl; B^{II} = Ca, Sr, Ba, Pb) exhibit ground-state splittings ($4E_{JT} \simeq 7900 \pm 800$ cm^{-1}) and distortions of the CuN_6 polyhedra ($\rho \simeq 0.27 \pm 0.05$ Å)[7,16] of similar magnitude, which vary considerably, however, due to the influence of differing cooperative Jahn–Teller forces.

The ligand field spectrum of $[Cu^{II}(ODACN)_2]Br_2$ is very interesting insofar as the lowest energy band has shifted from 7800 to ≃13 500 cm^{-1}, compared to the band of the compound with triaza ligands (Figure 1, spectrum III). This is a clear indication that the weaker oxygen ligator atoms occupy elongated axial positions, thus enhancing the Jahn–Teller distortion and inducing a more pronounced tetragonality than in the case of a complex with six identical nitrogen ligands. The second band at 18 300 cm^{-1} is expected to have the AOM energy $3e_\sigma^s$ (eq 1), if one neglects the π-antibonding contributions of the oxygen ligator atoms in the very weakly bonded axial positions of the strongly elongated $Cu^{II}N_4O_2$ octahedron. The energy parameter e_σ^s reflects the Cu–N bond lengths in the equatorial plane, and the corresponding overlap integral can be calculated by comparison with e_σ^s for the triaza complex: $S^2 = e_\sigma^s(\text{"}N_2O\text{"})/[e_\sigma^s(\text{"}N_3\text{"})]S(2.06\ Å)^2$. We derive Cu–N spacings of ≃2.00 Å, which are ≃0.06 Å smaller than those for the TACN complex and hint to very long axial bond lengths around 2.45 Å.

The reflection spectrum of $[Cu(TTCN)_2](ClO_4)_2$ is indicative of the presence of a Jahn–Teller distortion with the ground-state splitting $4E_{JT} = 7800$ cm^{-1}. The same splitting was observed for the corresponding triaza complex (Figure 1, spectra I and II). In contrast to the Ni^{2+} spectrum the charge-transfer region extends into the visible region down to about 18 000 cm^{-1}. We assign the shoulder at ≃17 000 cm^{-1} to the transitions $^2B_{1g} \rightarrow {}^2B_{2g}, {}^2E_g$. It will be shown in part II that the interpretation and assignment of the ligand field spectra are consistent with the available EPR evidence.

II. Cu^{2+} EPR Spectra. Single-crystal, powder, and solution EPR data for $[Cu(TACN)_2][Cu(CN)_3]_2$ have been reported[15] and are listed in Table II. The powder spectrum of $[Cu(ODACN)_2]Br_2$ shows very narrow signals of tetragonal symmetry, with $g_\parallel = 2.20_8$ and $g_\perp = 2.04_9$ ($\bar{g} = 2.10_2$). When the temperature is lowered to 130 K, a small anisotropy in the $g_\perp$ signal is resolved ($g_z = 2.20_4$, $g_y = 2.05_0$, $g_x = 2.04_5$; $\bar{g} = 2.09_9$), which is apparently due to the presence of the tiny trigonal ligand field component induced by the tridentate ligands (Figure 2). From the orbital contributions (u) to the g values, utilizing the energy of the ligand field transition $^2B_{1g}(^2E_g) \rightarrow {}^2B_{2g}, {}^2E_g(^2T_{2g})$ (D_{4h} symmetry) at $\delta E = 18\,300$ cm^{-1}, the spin–orbit coupling parameter $\zeta_0 = 830$ cm^{-1}, and eq 3 we obtain a covalency parameter k of 0.75_5, which is identical with the one for the triazacyclononane complex (Table II) and similar to the one reported for $Cu(terpy)_2^{2+}$ (0.78).[5] In the solid-solution (DMSO) EPR spectrum at 130 K (Figure 2) two component spectra are clearly visible, in which the $A_\parallel$ hyperfine splitting is nicely resolved. While

$$g_\parallel = g_0 + 8u - 7u^2 \qquad g_\perp = g_0 + 2u - 4u^2 \qquad u = \frac{k^2\zeta_0}{\delta E} \quad (3)$$

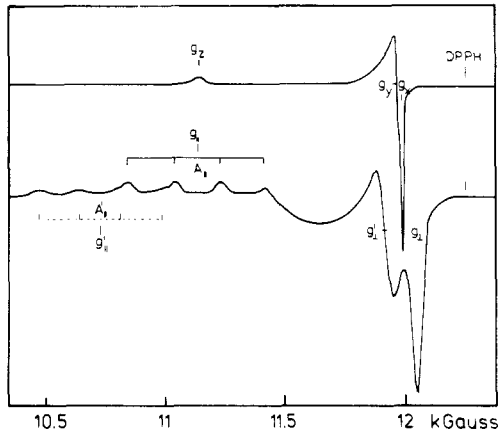

Figure 2. EPR powder (top; 130 K) and frozen-solution spectra (bottom; DMSO, 130 K) of $[Cu(ODACN)_2]Br_2$.

the spectrum with the dominating intensity corresponds to the one observed in the crystalline state ($g_\parallel = 2.20_5$, $g_\perp \simeq 2.04$), the second spectrum has much larger g values ($g_\parallel' \simeq 2.28$, $g_\perp' \simeq 2.06$). Due to the overlap in particular in the $g_\perp$ region only the $g_\parallel$ signal can be determined with high precision. We think that the second spectrum is caused by polyhedra in which only one of the weaker oxygen ligator atoms occupies an elongated axial position. In this case a ground-state splitting is expected, which is similar to that of the triazacyclononane complex because of a reduced axial elongation. Though the region between 4000 and 8000 cm^{-1} in the solution ligand field spectrum (DMSO) is obscured by the absorption of the solvent molecules and the tridentate ligand, there is some indication for a weak ligand field transition around 6000–6500 cm^{-1} (Figure 1, spectrum IV). If we adopt this energy as $4E_{JT}$ and choose $\delta E(^2B_{1g} \rightarrow {}^2B_{2g}, {}^2E_g) \simeq 14\,500$ cm^{-1}—at about 1500 cm^{-1} smaller energies than for $Cu(TACN)_2^{2+}$, mostly due to the smaller ligand field parameter Δ (see above)—we obtain (with $k = 0.76$) the g values (eq 3) $g_\parallel \simeq 2.27$ and $g_\perp \simeq 2.07$, which are very near to those observed for the additional species (Table II). From the well-resolved copper hyperfine splitting in the $g_\parallel$ signal of the trans-configurated species (Figure 2, $|A_\parallel| = 198 \times 10^{-4}$ cm^{-1}) we can deduce the mixing coefficient of the $d_{x^2-y^2}$ orbital in the B_{1g} ground-state molecular orbital

$$\Phi = \alpha d_{x^2-y^2} - \alpha' \sigma_{x^2-y^2} \quad (4)$$

by utilizing the equations[20]

$$A_\parallel = P[-\alpha^2(\kappa + {}^4/_7) + {}^3/_7(g_\perp - g_0) + g_\parallel - g_0]$$

$$A_\perp = P[-\alpha^2(\kappa - {}^2/_7) + {}^{11}/_{14}(g_\perp - g_0)]$$

$$A_{iso} = {}^1/_3(A_\parallel + 2A_\perp) = P[-\alpha^2\kappa + g_{iso} - g_0] \quad (5)$$

With $\kappa = 0.43$ and $P = 0.036$ cm^{-1}, which values are characteristic for the free Cu^{2+} ion, and assuming $A_\parallel$ to be negative,[20] we obtain $\alpha = 0.87_5$ (Table II). $A_\perp$ is not resolved in the spectra and calculated to be -27×10^{-4} cm^{-1}, while the dynamically averaged A_{iso} parameter should have a value of -82×10^{-4} cm^{-1}—in accord with the EPR spectra in DMSO solution ($|A_{iso}| = 83 \times 10^{-4}$ cm^{-1}). The mixing coefficient α for the triazacyclononane complex (Table

(20) Ozarowski, A.; Reinen, D. *Inorg. Chem.* **1985**, *24*, 3860.

II) is very similar to the one for the trans oxa diaza complex, though one would have expected a slightly lower value in the latter case because of reduced Cu–N bond lengths (see above). From the $|A_\parallel'|$ hyperfine constant in the additional EPR spectrum of Figure 2 ($\simeq 182 \times 10^{-4}$ G) an α coefficient $\simeq 0.90$ is deduced, which is larger than the one for the complex with both oxygen atoms in the strongly elongated axial positions. A smaller d-electron delocalization is indeed expected, because the equatorial bonds should be comparatively weaker in the presumed cis-configurated species. One oxygen ligator atom is present, and the distortion is considerably smaller.

The solution and frozen solution EPR spectra of $[Cu^{II}(TTCN)_2](ClO_4)_2$ yield the **g** and hyperfine tensor components, collected in Table II. The frozen-solution **g** tensor is in agreement with a $d_{x^2-y^2}$ ground state and hence is indicative of a tetragonally elongated octahedron (eq 3). A possible anisotropy of u due to a splitting of the π-antibonding $^2T_{2g}$ parent state and the influence of spin–orbit coupling effects from the sulfur ligands on the g values (which should be small) were not considered. The calculated covalency parameter is smaller than the one of the triaza analogue by a factor of $\simeq 0.7$ (Table II). From the measured $A_\parallel$ and A_{iso} hyperfine values and with $\kappa = 0.43$ and $P = 0.036$ cm^{-1} (eq 5) we obtained the mixing coefficient $\alpha = 0.74$ of the $d_{x^2-y^2}$ orbital in the $^2B_{1g}$ ground state. Consistent results are only obtained if $A_\parallel$, $A_\perp$, and A_{iso} are assumed to be negative. $A_\perp$ is not resolved in the spectra and is calculated to be $\simeq -20 \times 10^{-4}$ cm^{-1}. The σ covalency of the Cu–S bond is considerably larger than the one for the Cu–N bond ($\alpha_S/\alpha_N = 0.85_5$). Because the covalency parameter k on the other hand is proportional to $\alpha\beta$ (β is the mixing coefficient of the t_{2g} molecular orbitals in the π-antibonding $^2B_{2g}$ and ^2E_g states) and the triaza ligand a pure σ donor with $\beta_N = 0$, one may calculate $\beta_S \simeq 0.85$. Though this value is only a rough estimate, we have evidence for the presence of significant π contributions to the Cu–S bond. Referring to the AOM calculations we have performed on the basis of the spectroscopic data for the Cu(II)–triaza complex (eq 1), we can similarly estimate e_σ and e_π parameters for the trithia complex. Adopting the structural data reported for $[Cu^{II}S_6\text{-}18\text{-crown-}6](pic)_2$ (pic = picrate) [Cu–S = 2.63 (2×), $\simeq$2.36 Å (4×),[21] $\rho = 0.31$ Å], which has **g**- and **A**-tensor components nearly equivalent to those of our compound, we calculate e_σ^s and e_σ^l to be 6000 and 3350 cm^{-1}, respectively. Again tabulated overlap integrals were used, and for E_{ds} the same energy was chosen as found for the triaza complex (2600 cm^{-1}). The calculated e_σ^0 parameter for the average bond length of 2.45 Å (5000 cm^{-1}) is larger than the one for the triaza analogue (4400 cm^{-1}). Finally we can roughly estimate e_π^0 from the modified eq 1, $E_{T_2} \simeq 3e_\sigma^s - 2e_\pi^0$, which takes into account that only one p orbital of each S atom can take part in π bonding. We obtain $e_\pi^0 \approx 500$ cm^{-1}. The higher degree of covalency of the transition-metal–sulfur bond as compared to that of the triaza ligand is also in accord with the decrease of the nephelauxetic ratio, observed for Ni^{2+}.

The X- and Q-band powder spectra of solid $[Cu^{II}(TTCN)_2](ClO_4)_2$, measured at temperatures between 5 and 300 K, are rather complicated, because exchange narrowing between different CuS_6 entities in the unit cell obscures the molecular **g** tensor. The average g value is the same as the one in solution, however, and the distinct anisotropy of the EPR signal even at 298 K proves that the Cu^{II} polyhedra are still statically Jahn–Teller distorted at 298 K. This is in contrast to the X-ray single-crystal study of $[Cu^{II}(TTCN)_2](BF_4)_2 \cdot 2CH_3CN$ at 298 K, which finds nearly undistorted CuS_6 polyhedra.[22] Apparently the Jahn–Teller distortion is dynamic already at room temperature in this case. It is well-known, however, that the transition from the static to the dynamic Jahn–Teller effect may occur in different temperature ranges for the same transition-metal complex, depending on finer details such as different counterions or the presence of solvent molecules in the unit cell.[5,16,23] Such a transition often occurs

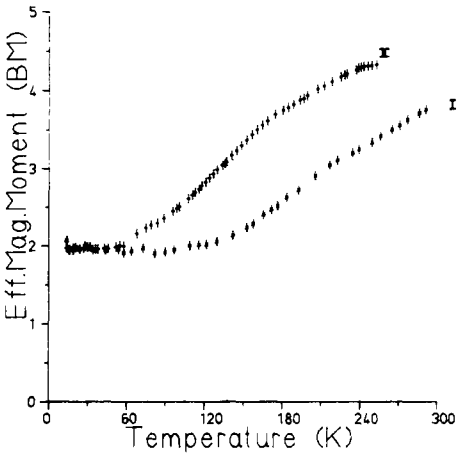

Figure 3. μ_{eff} versus temperature diagrams from susceptibility measurements (Foner magnetometer; heating curves) for $Co[ODACN]X_2$: (I) X = Br^-; (II) X = I^-.

continuously over a wide temperature range of 200 K and more, implying partly dynamically averaged molecular geometries at intermediate temperatures.[15]

III. Co^{2+} Ligand Field Spectra and Magnetic Properties. The Co^{2+} ion in the compound $[Co(TACN)_2]I_2 \cdot 2H_2O$ is high-spin configurated, as is deduced from magnetic measurements and from the average Co–N bond length,[14] which closely resembles the average Cu–N spacings in corresponding Cu^{2+} complexes[15] [ionic radii: Cu^{2+} and Co^{2+} (high spin), $\simeq$0.73 Å; Co^{2+} (low spin), 0.65 Å[24]]. The reflectance spectrum and the reported ligand field spectrum in water (reducing conditions)[14] agree with these observations. The two bands of dominating intensity at 11 200 and 21 500 cm^{-1} can be assigned to the transitions $^4_aT_{1g} \rightarrow {}^4T_{2g}$ and $^4_bT_{1g}$. The deduced ligand field parameters are $\Delta = 12\,000$ cm^{-1} ($e_\sigma = 4000$ cm^{-1}) and $B = 780$ cm^{-1} (with $B_0 = 970$ cm^{-1}: $\beta = 0.82_5$), consistent with the values for Ni^{2+} (Table I). The lowering of the ground state $^4_aT_{1g}$ by spin–orbit splitting effects was included ($\zeta = 360$ cm^{-1}). The third main band $^4_aT_{1g} \rightarrow {}^4A_{2g}$, which corresponds to a two-electron jump and hence should be of low intensity, is expected at $\simeq$23 000 and not resolved in the spectrum. The weak shoulder at $\simeq$18 400 cm^{-1} can be fitted reasonably well by assuming it to be the quartet–doublet transition $^4_aT_{1g} \rightarrow {}^2_aT_{1g}$, which is usually detected in octahedral Co^{2+} spectra ($C/B = 4.3_5$).[25] The energy of the $^2_aE_g$ term, which would be the ground state in case of low-spin Co^{2+}, is approximately

$$E_{4,2}(O_h) \simeq 4B + 4C - \Delta \qquad (6a)$$

The estimated high-spin–low-spin energy separation of $\simeq$4700 cm^{-1} is only a rough estimate, however, because configuration interaction between the two $^4T_{1g}$ terms and between the five ^2E_g states as well as spin–orbit coupling are not taken into account.

Interestingly enough the corresponding $Co(terpy)_2^{2+}$ salts are mostly low-spin configurated, obviously due to a lower B value of $\simeq$750 cm^{-1},[26] consistent with the results for Ni^{2+}. In contrast to the nonbonding (or π-antibonding) $^4_aT_{1g}$ ground state the excited σ-antibonding $^2_aE_g$ state ($t_{2g}^6e_g^1$) is highly Jahn–Teller unstable. Induced by a tetragonal elongation of the octahedron, it may undergo an appreciable Jahn–Teller splitting $4E_{JT}$, which eventually stabilizes a low-spin ground state[16] as is easily estimated from eq 6b for D_{4h} symmetry. From the reported ligand field

$$E_{4,2}(D_{4h}) \simeq 4B + 4C - \Delta - 2E_{JT} \qquad (6b)$$

parameters ($\Delta \approx 13\,500$ cm^{-1}, $\beta \simeq 750$ cm^{-1}, $4E_{JT} \simeq 7500$ cm^{-1})[26]

(21) Hartmann, J. A. R.; Cooper, S. R. *J. Am. Chem. Soc.* **1986**, *108*, 1202.
(22) Setzer, W. A.; Ogle, C. A.; Wilson, G. S.; Glass, R. S. *J. Am. Chem. Soc.* **1983**, *22*, 266.
(23) Reinen, D. In *Proceedings of the Second Conference on Copper Coordination Chemistry, Albany, NY, 1984*; Karlin, K. D., Zubieta, J., Eds.; Adenine: Guilderland, NY, 1985; Vol. I, p 247.
(24) Shannon, R. D.; Prewitt, C. T. *Acta Crystallogr., Sect. B: Struct. Crystallogr. Cryst. Chem.* **1969**, *B25*, 925.
(25) Reinen, D. *Monatsh. Chem.* **1965**, *96*, 730.
(26) Kremer, S.; Henke, W.; Reinen, D. *Inorg. Chem.* **1982**, *21*, 3013.

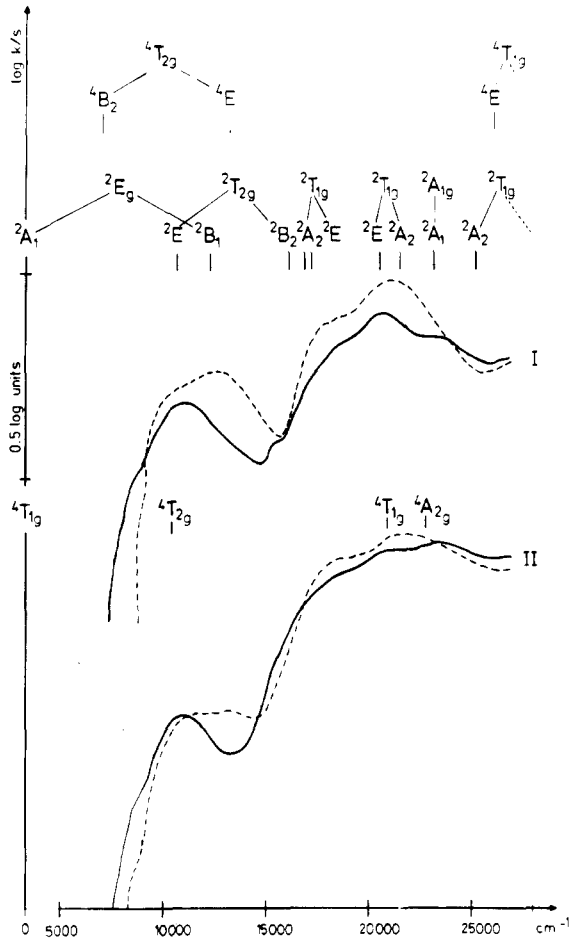

Figure 4. Reflection spectra of $[Co(ODACN)_2]X_2$ at 298 K (—) and 5 K (---): (I) X = I^-; (II) X = ClO_4^-. The assignment of spectrum I at 5 K (low-spin ground state; D_{4h}, elongation) was accomplished with fitting parameters Δ = 12 800 cm^{-1}, $4E_{JT}$ = 13 600 cm^{-1}, B = 800 cm^{-1}, and $C/B = 4.3_5$; spectrum II (and I) at 298 K (high-spin ground state, O_h) was assigned with Δ = 11 800 cm^{-1} and B = 800 cm^{-1} ($\zeta \simeq 360$ cm^{-1}). (For the tetragonal assignment the octahedral parent terms are also given; below 9000 cm^{-1} absorptions from the ligand are visible.)

we calculate a negative energy separation $E_{4,2}(D_{4h})$ and hence a low-spin ground state. An increase of B by about 50 cm^{-1} and a decrease of Δ by about 1500 cm^{-1} [$\Delta \simeq 12000$ cm^{-1} (high spin), 13 500 cm^{-1} (low-spin)], which are the essential parameter changes when terpy is substituted by TACN, would render $E_{4,2}(D_{4h})$ positive and leave the complex in the high-spin state. The hexanitrocobalt(II) entities in compounds $A^I_2M^{II}Co(NO_2)_6$ (A^I = K, Rb; M^{II} = Sr, Ba) are low spin,[16,27] with a larger $4E_{JT}$ energy (8400 cm^{-1}) than observed for the terpyridine complexes.

The complexes $[Co(ODACN)]X_2$ (X = Br^-, I^-) possess low-spin ground states with a magnetic moment of 1.96 μ_B for $T \lesssim 60$ K (I^-) and $T \lesssim 120$ K (Br^-) (Figure 3), which corresponds to $S = {}^1/_2$ with a small orbital contribution (g = 2.26). The 5 K reflection spectra are assigned on the basis of an elongated D_{4h} symmetry with a $^2A_{1g}$ ground state (see the EPR data in part IV) and the ligand field parameters Δ = 12 800 cm^{-1}, $4E_{JT}$ = 13 600 cm^{-1}, B = 800 cm^{-1}, $C/B = 4.3_5$, with use of the energy matrices in ref 28 (Figure 4). π bonding was assumed to be negligible.[29] Without stressing the accuracy of Δ and B too much, the chosen set of parameters in general nicely reproduces the intensity distribution within the two double-peaked bands. The Δ parameter is about 1500 cm^{-1} larger than that expected for a high-spin complex, while the splitting of the ^2E_g ($t_{2g}^6e_g^1$) ground state due

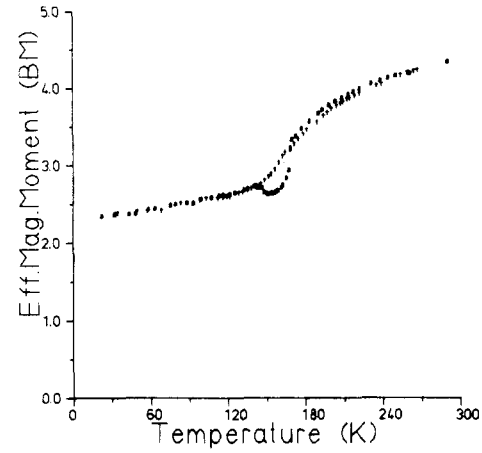

Figure 5. μ_{eff} versus temperature diagram for $[Co(ODACN)_2](ClO_4)_2$. (The curve with a minimum refers to heating from 4 to 300 K; the smooth curve corresponds to cooling the sample from 300 to 4 K.)

to the combined action of the Jahn–Teller effect and the weaker O ligator atoms in the axial positions is comparable to that of Cu^{2+}. The first excited quartet states—$^4_aA_{2g}$ and $^4_aE_g$ from the $^4_aT_{1g}$ parent term—are calculated to have the energies 3050 and 2400 cm^{-1}, respectively, in good agreement with the estimation from eq 6b. In comparison with $Co(TACN)_2^{2+}$ it is hence the comparatively much larger tetragonal distortion that finally stabilizes a low-spin ground state for the ODACN complexes.

The magnetic moments μ_{eff} of the two considered compounds exhibit marked temperature dependencies (Figure 3). For X = I^- (Br^-) the μ_{eff} values start to increase with respect to those that characterize a pure low-spin ground state at about 60 (120) K and—after characteristic turning points around 140 (200) K—reach 4.4 and 3.7 μ_B at 293 K. The former value is not far from the magnetic moment for octahedral high-spin Co^{2+} complexes and hints toward a rather small or even slightly negative quartet–doublet separation energy $\delta_{2,4}$,[30] which determines the Boltzmann distribution over the $S = {}^1/_2$ and $S = {}^3/_2$ states. The low-spin state is stabilized by elastic forces between the distorted polyhedra in the unit cell. A larger population of excited quartet states, which are not affected by the Jahn–Teller effect significantly, will destroy the cooperative interactions and lead to a decrease of $\delta_{2,4}$ with increasing temperature. This will induce an even larger population of excited quartet states and may explain the turning points in the μ_{eff}–T dependencies (Figure 3). The $\delta_{2,4}$ energy separation seems to be slightly larger for the bromide compared to that for the iodide salt.

The temperature dependence of μ_{eff} for the compound $[Co(ODACN)_2](ClO_4)_2$ is very different. While the room-temperature magnetic moment of $\simeq$4.4 μ_B is practically identical with the one for the iodide, the observed μ_{eff} values at $T \lesssim 50$ K are $\simeq$2.5 μ_B, significantly deviating from the low-spin limit (Figure 5). Obviously high- and low-spin Co^{2+} are present side by side even at 4 K, hinting toward a vanishing $\delta_{2,4}$ separation energy already at very low temperatures. Interestingly enough the complexes $Co(terpy)_2X_2$ also undergo high-spin–low-spin equilibria with an increase of $\delta_{2,4}$, if X changes from ClO_4^- over I^- to Br^-.[26] As in the discussed case, the perchlorate shows an anomalous behavior. The μ_{eff}–T curve in Figure 5 shows some special features. If the susceptibility data are collected with heating of the sample from 4 K, a minimum is always observed in the μ_{eff}–T curve, the position of which differs slightly from measurement to measurement. Only cooling from 300 to 4 K yields reproducible results in the whole temperature range. Possibly the vibronic interaction

(27) Backes, G.; Reinen, D. *Z. Anorg. Allg. Chem.* **1975**, *418*, 217.
(28) Perumareddi, J. R. *Coord. Chem. Rev.* **1969**, *4*, 73.
(29) As before, only the Jahn–Teller splitting of the σ-antibonding e_g molecular orbitals was taken into account, while the splitting of the π-antibonding t_{2g} levels was considered to be negligible.
(30) $-E_{4,2}(D_{4h})$ is the Franck–Condon energy separation between the potential surfaces, describing the excited quartet and the doublet ground state (eq 6b), while $\delta_{2,4}$ is the energy difference between the lowest vibronic levels of the two potential curves. $\delta_{2,4}$, which may be much smaller than $-E_{4,2}(D_{4h})$, clearly determines the thermal occupation mechanism, which gives rise to the temperature dependence of the magnetic moments and EPR signals.

Table III. EPR Data (Hyperfine Tensor Components in 10^{-4} cm^{-1}) and Bonding Parameters of Complexes $[Co(ODACN)]X_2$ (X = I^-, Br^-) (A) and $[Co^{II}(TTCN)_2](ClO_4)_2$ (B) in the Solid State (i) and in DMF Solution (ii)

	temp, K	g_x	g_y	g_z	$A_\parallel$	A_{iso}	$A_\perp$	α
A(i)	4.2		2.27_9	2.05_0				
A(ii)	4.2		2.31_6	2.03_4	84		$\simeq 0$	0.93
B(i)	4.2		2.11_8	2.02_0				
	77	2.11_7	2.09_6	2.04_1				
	298	2.10_8	2.09_1	2.05_9				
B(ii)	150		2.12_1	2.01_9	33		−72	
	280		2.09			−38		0.84

between the potential surfaces of high- and low-spin Co^{2+} is particularly small for the perchlorate and prevents relaxation between doublet and quartet states at sufficiently low temperatures.[31] The evidence from the reflection spectra supports the magnetic results (Figure 4). While the 5 K spectrum of the iodide reflects low-spin Co^{2+}, the 298 K spectra of the perchlorate and iodide are predominantly governed by transitions due to high-spin Co^{2+}. With a Δ value of $\simeq 11\,800$ cm^{-1}—only slightly lower than for the triaza complex—and $B = 800$ cm^{-1} ($\zeta = 360$ cm^{-1}), one can indeed reproduce the energy of the lowest $^4_aT_{1g} \rightarrow {}^4T_{2g}$ band (10 900 cm^{-1}). The transitions to the $^4_bT_{1g}$ and $^4A_{2g}$ terms, which are expected at $\simeq 21\,700$ and 22 700 cm^{-1}, are not completely resolved in the broad higher energy band and are apparently obscured by absorptions due to low-spin Co^{2+}. The spectra of the perchlorate and iodide at 5 K reflect increasing band intensities from low-spin Co^{2+}, compared with the room-temperature spectra. The DMF solution spectra at 298 K are mainly characteristic for high-spin Co^{2+}.

$[Co(TTCN)_2](ClO_4)_2$ possesses a low-spin ground state between 4 and 300 K (part IV). Though the reflection spectrum is not well-resolved, ligand field parameters $4E_{JT} \simeq 7000$ cm^{-1} and $\Delta \simeq 13\,500$ cm^{-1}, close to the expected values, can be deduced. If one follows the trend given by Ni^{2+} in the alternative TACN and TTCN surroundings, a reasonable choice for B is 730 cm^{-1}. With these parameters the quartet–doublet separation $E_{4,2} = -1400$ cm^{-1} is estimated (eq 6b). The larger covalency of TTCN with respect to that of the TACN ligand, apparent through the larger nephelauxetic effect (decrease of B by 70 cm^{-1}), is mainly responsible for the change from the high- to the low-spin configuration.

IV. Co^{2+} EPR Spectra. The EPR spectrum of $[Co(TACN)_2]I_2 \cdot 2H_2O$ at 4.2 K is strongly anisotropic, with two broad signals at g values around 10 ($g_\parallel$) and 2 ($g_\perp$), which are indicative for high-spin Co^{2+} in a distorted octahedral coordination. Already at 80 K it becomes too broad for observation. The crystal structure of $[Co(TACN)_2]I_2 \cdot 2H_2O$ indeed yields a small tetragonal elongation of the CoN_6 octahedra.[14] This symmetry effect could be caused by a small vibronic admixture of wave functions from the highly Jahn–Teller unstable $^2_aE_g$ term into the ground state.

The low-temperature EPR spectra of $[Co(ODACN)_2]X_2$ (X = Br^-, I^-) in the solid state and in solution (Figures 6 and 7; Table III) are in accord with a $^2A_{1g}$ ($\hat{=}d_{z^2}$) ground state (low-spin configuration, D_{4h} elongation), for which the following g values are expected[32,33]—if spin–orbit interactions with excited doublet and quartet terms are taken into account up to second and third order, respectively:

$$g_\parallel = g_0 + 2u_{2,4}^2 \qquad g_\perp = g_0 + 6u + 2u_{2,4}^2 \qquad (7)$$

$u = 0.047$ summarizes over the former and $u_{2,4} = -k^2\zeta_0/E_{4,2} = 0.125$ (values from the frozen-solution **g** tensor) comprises the latter orbital contributions. With the free ion LS coupling constant $\zeta_0 = 540$ cm^{-1} and with the covalency factor $k \simeq 0.8$, which is somewhat larger than the one for Cu^{2+} in the same surroundings (see below), a quartet–doublet separation $E_{4,2}(D_{4h}) \simeq -2800$ cm^{-1} is estimated, which is consistent with the value from the ligand field calculation. In the $g_\parallel$ signal of the frozen-solution spectra (Figure 6) the hyperfine structure due to the nuclear spin $I = {}^7/_2$ of Co^{2+} is clearly seen. In contrast to the results for Cu^{2+} we could

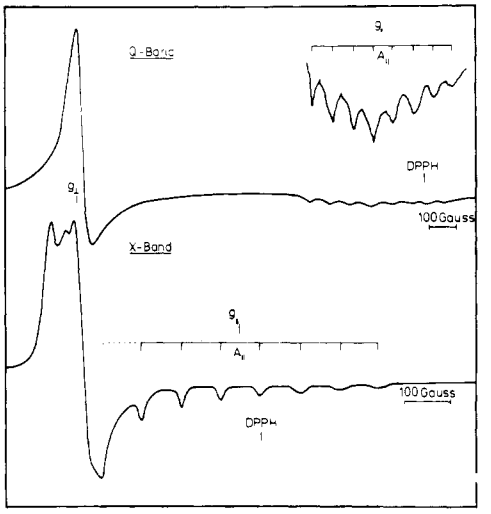

Figure 6. EPR frozen-solution spectra of $[Co(ODACN)_2]I_2$ (DMF, 130 K). (The splitting of the $g_\perp$ signal in the X-band spectrum is due to the specific angular dependencies of the $A_\parallel$ hyperfine components and not to an $A_\perp$ hyperfine structure, which can be demonstrated by spectral simulation.)

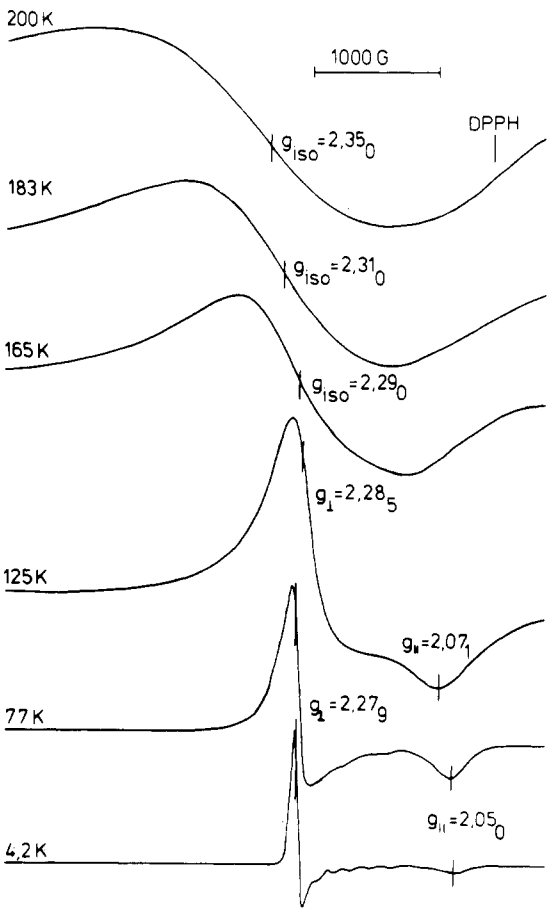

Figure 7. Temperature dependence of the EPR spectra of solid $[Co(ODACN)_2]I_2$ (Q-band). The averaged g value changes from 2.20_1 (4.2 K) to $\simeq 2.6$ (240 K).

(31) Bacci, M. *Inorg. Chem.* **1986**, *25*, 2322.
(32) Lacroix, R.; Hoechli, U.; Müller, K. A. *Helv. Phys. Acta* **1964**, *37*, 627.
(33) McGarvey, B. R. *Can. J. Chem.* **1975**, *53*, 2498.

not detect an additional spectrum caused by a species with only one oxygen atom in the axial positions. Presumably this entity would be high-spin configurated and hence should only be observable at very low temperatures. A reduction of $4E_{JT}$ from 13 500 to 7500 cm^{-1} would indeed be sufficient to yield a high-spin ground state (eq 6b).

The hyperfine tensor components for the $^2_aA_{1g}$ (d_{z^2}) ground state of octahedral Co^{2+}—if third-order orbital contributions are included only for the $^2_aA_{1g}(^2E_g)$–$^4_aA_{2g}$, $^4_aE_g(^4T_{1g})$ interactions (as in eq 7)—are given by[33,34]

$$A_{\parallel} = P[\alpha^2(\kappa + {}^4/_7) - {}^2/_7 u - {}^4/_7 u_{2,4} - {}^{38}/_{63} u_{2,4}{}^2]$$

$$A_{\perp} = P[\alpha^2(\kappa - {}^2/_7) + {}^{43}/_7 u + {}^2/_7 u_{2,4} - {}^{50}/_{63} u_{2,4}{}^2]$$

$$A_{iso} = P[\alpha^2\kappa + 4u - {}^{46}/_{63} u_{2,4}{}^2] \quad (8)$$

The $A_{\parallel}$ parameter (84×10^{-4} cm^{-1}) can be deduced directly from the frozen-solution spectrum (Figure 6), while we could show by simulation of the experimental Q- and X-band spectra that $A_{\perp}$ is nearly vanishing (Table III). With the reported free ion dipolar splitting constant $P = 0.0254$ cm^{-1} [33] and eq 8 we estimate the isotropic Fermi hyperfine interaction parameter $\kappa = -0.08$ and the mixing coefficient $\alpha = 0.93$ [$\phi(^2A_{1g}) = \alpha d_{z^2} - \alpha' \sigma_{z^2}$]. Unfortunately A_{iso} could not be resolved in the liquid-solution spectra, because the signals become too broad at higher temperatures (see below). κ deviates considerably from the value reported for the free Co^{2+} ion ($\kappa_{3d} = -0.33$).[33,35] The deviation can be accounted for by $3d_{z^2}$–4s mixing effects, which are usually significant in the case of octahedral Co^{2+} complexes, in particular for strongly axially elongated and square-planar coordinations.[33,35] The 4s admixture into the $^2A_{1g}$ (d_{z^2}) ground-state MO leads to a contribution of sign opposite to that of κ, which is otherwise negative for Co^{2+} and describes the spin polarization of the d electrons on the filled metal s orbitals. In the presence of 4s admixing the term $\eta^2\kappa_{4s}$ has to be taken into account, where κ_{4s} is 4.85 for Co^{2+} and η is the coefficient of the 4s admixture into the $3d_{z^2}$ ground state. η can be obtained from eq 9.[35] The calculated fractional occupancy

$$\eta^2 \simeq \alpha^2(\kappa - \kappa_{3d})/\kappa_{4s} \quad (9)$$

of the 4s orbital by the unpaired electron is $\eta^2 \simeq 0.045 \triangleq 4.5\%$, in good agreement with various other strongly elongated octahedra with low-spin Co^{2+}.[33,35,36] In the rare cases in which Cu^{2+} is found in a compressed octahedron and hence also forced into a $^2A_{1g}$ ground state of predominant d_{z^2} character, similar changes of κ due to $3d_{z^2}$–4s mixing occur.[37] The energetic effect of this mixing, which enhances the splitting of the octahedral ^2E_g state due to a tetragonal elongation for Co^{2+} (and Cu^{2+}) has been discussed above (AOM treatment of Cu^{2+} ligand field spectra: parameter E_{ds}). It has not been included in the ligand field calculation for Co^{2+} (Figure 4), however, in order to limit the number of adjustable parameters. The mixing coefficient $\alpha \simeq 0.93$ is considerably larger than those for Cu^{2+} with TACN and ODACN (Tables II and III), in accord with the different ground state. In an elongated octahedron the overlap of the ligand orbitals with a $d_{x^2-y^2}$ orbital is indeed expected to be more effective than with d_{z^2}, which has most of its electron density in the directions of the long metal to ligand bonds. Though the accuracy of α and κ should not be overemphasized, because $A_{\perp}$ could not be measured directly and eq 8 is slightly simplified,[34] the observed trends are certainly correct and are in line with the parameters for the TTCN complexes, discussed below.

The EPR spectra of the powder compounds are strongly temperature dependent. In the case of the iodide drastic changes of the spectra occur above 140 K—in the temperature region of the turning point in the μ_{eff}–T curves (Figures 3 and 7). The anisotropic spectrum becomes broader, and the average g values increase significantly. Already at 170 K the signals are so broad that possible anisotropies are no longer revealed. For the bromide complex one observes similar changes, but the broadening effects and the increase of the g values are shifted toward higher temperatures, consistent with the results from the magnetic susceptibility measurements. The signals are anisotropic up to 220 K in this case. The thermal equilibrium between doublet and quartet states induces an increasing population of excited quartet levels with increasing temperature. Due to fast relaxation between the doublet and quartet states the anisotropy of the signals, which is characteristic only for doublet ground states, is reduced and the line width becomes larger. The g values shift toward those that are characteristic for high-spin Co^{2+}. Very similar observations have been made for salts of the $Co(terpy)_2^{2+}$ cation, and a theoretical model has been developed on the basis of EPR, magnetic, ligand field, and structural data.[26]

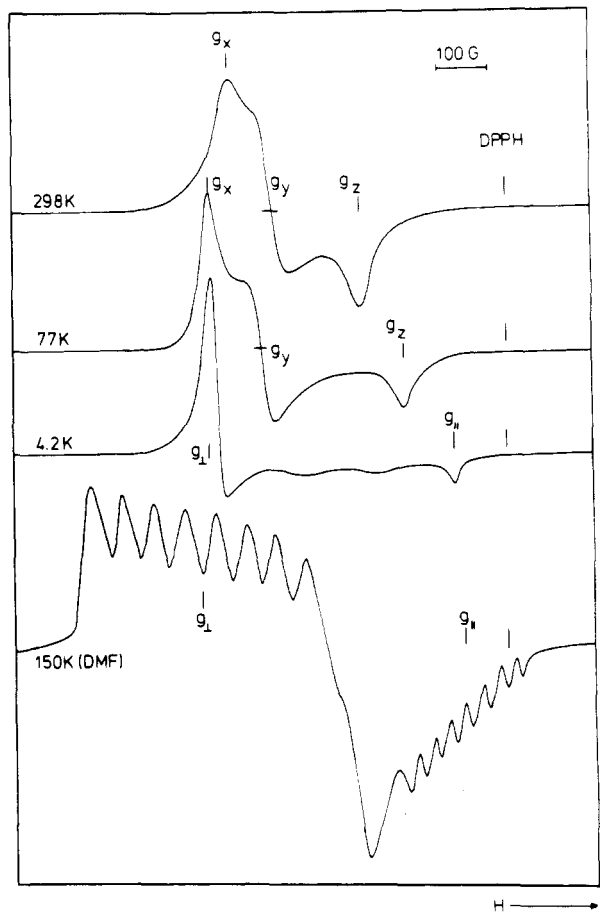

Figure 8. EPR Q-band spectra of $[Co(TTCN)_2](ClO_4)_2$ in solid solution and as a powdered solid. (The weak signals around $g = 2.05$ and 2.08 in the 4.2 K spectrum are presumably due to exchange coupling effects.)

The low-spin EPR signals of the perchlorate exhibit a temperature dependence very similar to that measured for the iodide (Figure 7), and the transition to broad spectra with higher g_{iso} values occurs at similar temperatures. Below 50 K high-spin EPR signals are observed beside those of low-spin Co^{2+}, in agreement with the susceptibility data. Obviously fast relaxation between doublet and quartet states, which averages the EPR spectra, only occurs above this temperature.

The EPR solution and powder spectra of $[Co(TTCN)_2](ClO_4)_2$ between 4.2 and 298 K (Figure 8) are those expected for a low-spin d_{z^2} ground state, with no indication of a significant occupation of quartet states at higher temperatures. From the observed g values of the frozen-solution spectrum (Table III) we obtain $u = 0.01_7$ and $u_{2,4} = 0.095$ (eq 7). With the covalency parameter $k \simeq 0.6$—somewhat larger than for Cu^{2+} (Table II)—the high-spin–low-spin separation is calculated to be $E_{4,2}(D_{4h}) \approx -2000$ cm^{-1}, similar to the estimation from the ligand field data.

(34) We have additionally used the following simplifications in McGarvey's eq 27–30:[33] $c_3' \cong c_1 \equiv u$ and $c_3 \cong c_5 \equiv u_{2,4}$.
(35) Labanze, G.; Raynor, J. B. *J. Chem. Soc., Dalton Trans.* **1980**, 2388; **1981**, 590.
(36) Rockenbauer, A. R.; Budó-Zakoryi, E.; Sinándi, L. J. *J. Chem. Soc., Dalton Trans.* **1975**, 1729.
(37) Hitchman, M. A.; McDonald, R. G.; Reinen, D. *Inorg. Chem.* **1986**, *25*, 519.

The tetragonal **g** tensor of the powder spectrum at 4.2 K becomes markedly orthorhombic when the temperature is raised. In the region up to $T \simeq 140$ K one $g_\perp$ component and the $g_\parallel$ signal approach each other. Above this temperature also the second component of $g_\perp$ moves toward the average g value. We think that at lower temperatures mainly the long Co–S bond lengths and two of the short Co–S bond lengths start to equilibrate ("planar dynamics"),[16] while the remaining short Co–S spacings take part in the averaging process only at higher temperatures. At 298 K the geometry is not yet completely dynamically averaged, and still significant differences in the Co–S bond lengths are expected to occur. Interesting in this connection is the crystal structure of $[Co(TTCN)_2](BF_4)_2 \cdot 2CH_3NO_2$, which contains compressed CoS_6 octahedra [Co–S = 2.36 Å (4×), 2.24 Å (2×)].[22] This finding does not necessarily imply a $d_{x^2-y^2}$ ground state but may indicate a "planar dynamic" effect similar to that suggested for the perchlorate complex between 4.2 and ≃140 K. Motional narrowing processes can indeed extend over a wide temperature range as was found for $[Cu(TACN)_2][Cu(CN)_3]_2$ for example and rationalized on the basis of structural and spectroscopic single-crystal data in terms of a continuous transition from a static to a dynamic Jahn–Teller effect between 150 and 350 K.[15] Comparable to the case for Cu^{2+}, the coordination geometry of low-spin Co^{2+}, which is revealed in a structure analysis at 298 K, may represent any conformation on the distortion path between the static limit of a tetragonally elongated and a completely dynamically averaged octahedron—depending on the specific packing conditions in the unit cell (presence of solvent molecules, etc.). The static limit is apparently realized in the structure of $[Co(TTN)_2](BF_4)_2 \cdot CH_3NO_2$ with the tridentate 2,5,8-trithianonane ligand, which shows strongly elongated octahedra [Co–S = 2.61 Å (2×), 2.25 Å (4×); $\rho = 0.42$ Å].[38] Single-crystal EPR and structural analyses on $[Co(TTCN)_2]^{2+}$ with various counterions are in progress, in order to obtain a better understanding of the fluxionality of the CoS_6 polyhedra in dependence on temperature.

The solution and frozen-solution spectra exhibit well-resolved hyperfine structures in both the $g_\parallel$ and $g_\perp$ signals and—as we could prove by simulations—reflects a tetragonal **g** tensor (Table III, Figure 8). $g_\parallel$ and $g_\perp$ are identical with those of the solid perchlorate salt at 4.2 K. It is surprising, however, that $|A_\parallel|$ is smaller by a factor of 2 than $|A_\perp|$. With the free ion dipolar splitting constant $P = 0.0254$ cm^{-1} the observed hyperfine constants in liquid and solid solution can be ideally fitted to eq 8, if the isotropic Fermi hyperfine interaction parameter κ and the mixing coefficient α are chosen to be −0.29 and 0.84, respectively, and the signs of the hyperfine parameters are as in Table III. κ is nearly of the magnitude reported for the free Co^{2+} ion ($\kappa_{3d} = -0.33$), and hence the reduction of κ due to $3d_{z^2}$–4s mixing is very small. From eq 9 we calculate $\eta^2 = 0.006 \triangleq 0.6\%$. This result matches with systematic studies on pseudooctahedral low-spin Co^{2+} complexes, which find decreasing η values, if the metal to ligand covalency increases[35] and the tetragonal elongation[33] diminishes. Compared to the case for $[Co(ODACN)_2]^{2+}$ complexes with more electronegative ligands and a considerably larger distortion ($\rho \simeq 0.52$ Å; $\eta^2 \simeq 0.045$) the trend toward a smaller 4s admixing is hence expected. The larger covalency is also reflected by a considerable decrease of α from 0.93 to 0.84. The mixing coefficient is also larger than α of the corresponding $[Cu(TTCN)_2]^{2+}$ complex (Tables II and III), caused by the different ground state, as discussed above.

(38) Hartmann, J. A. R.; Hintsa, E. J.; Cooper, S. R. *J. Am. Chem. Soc.* **1986**, *108*, 1208.

Conclusions

The spectroscopic and magnetic investigation of octahedral complexes of Cu^{2+} and Co^{2+} with the tridentate triazacyclononane, oxadiazacyclononane, and trithiacyclononane ligands brought some interesting results concerning the bonding properties.

(a) The trithia ligand induces a stronger σ covalency than the triaza analogue, as is directly reflected by the bonding parameters deduced from the EPR hyperfine structure. Because of significant π contributions to the M–S bonds, the Δ parameter is about the same for both ligands, however. Numerical values for the AOM parameters e_σ and e_π could be deduced.

(b) Cu^{2+} and low-spin Co^{2+} induce strong Jahn–Teller effects. The ground states are $d_{x^2-y^2}$ and d_{z^2} for the d^9 and low-spin d^7 cations, respectively, and in both cases the octahedra undergo considerable tetragonal elongations. The transition from the static to the dynamic distortion usually covers a wide temperature range. The room-temperature structure quite often yields only weakly distorted octahedra, because the bond lengths are partly dynamically averaged.

(c) While the triaza complex of Co^{2+} is high-spin configurated, the trithia complex has a low-spin ground state. The spin change is mainly caused by the smaller nephelauxetic B parameter of the latter complex as the result of the increased covalency. The substitution of the triaza by the oxa diaza ligand in the Co^{2+} complexes leads to doublet ground states, because the low-spin configuration is additionally stabilized by the much greater tetragonal elongation of the CoN_4O_2 octahedra. Because of rather small doublet–quartet separation energies temperature-dependent high-spin–low-spin equilibria are observed, however. The perchlorate salt behaves anomalously, because high-spin Co^{2+} is observed beside low-spin species even at 4.2 K.

Acknowledgment. Financial support of this work by the Deutsche Forschungsgemeinschaft and the Fonds der Chemischen Industrie is gratefully acknowledged.

Registry No. ODACN, 80289-59-4; $[Co(ODACN)_2](ClO_4)_2$, 110613-21-3; $[Co(ODACN)_2]I_2$, 110613-22-4; $[Co(ODACN)_2]Br_2$, 110613-26-8; $[Co(TACN)_2]I_2$, 110613-23-5; $[Cu(TTCN)_2](ClO_4)_2$, 110613-24-6; $[Co(TTCN)_2](ClO_4)_2$, 97465-54-8; $[Cu(ODACN)_2]Br_2$, 110613-25-7; $Ni(NH_3)_6^{2+}$, 15365-74-9; $Ni(en)_3^{2+}$, 15390-99-5; $Ni(TACN)_2^{2+}$, 59034-11-6; $[Cu(TACN)_2](ClO_4)_2$, 60296-53-9; *N,N'*-bis(*p*-tolylsulfonyl)-4,7-diaza-1-oxacyclononane, 60147-22-0.